Interactions between luminance steps and luminance textures for boundary segmentation

Abbreviated Title: Interactions between luminance cues

Christopher DiMattina [1,*]

[1]Computational Perception Laboratory & Department of Psychology
Florida Gulf Coast University, Fort Myers, FL, USA 33965-6565

***Corresponding Author:**
Christopher DiMattina
Whitaker Hall Room 215
Florida Gulf Coast University
10501 FGCU Blvd S.
Fort Myers, FL 33965-6565

Email: cdimattina@fgcu.edu
Web: http://itech.fgcu.edu/faculty/cdimattina/
Tel: (239)-590-1513

Conflict of Interest: The authors declare no competing financial interests.

Acknowledgements: We thank FGCU undergraduates in the Computational Perception Lab for help with data collection.

ABSTRACT

In natural scenes, two adjacent surfaces may differ in mean luminance without any sharp change in luminance at their boundary, but rather due to different relative proportions of light and dark regions within each surface. We refer to such boundaries as *luminance texture boundaries* (LTBs), and in this study we investigate interactions between luminance texture boundaries and luminance step boundaries (LSBs) in a segmentation task. Using a simple masking paradigm, we find very little influence of LSB maskers on LTB segmentation thresholds. Similarly, we find only modest effects of LTB maskers on LSB thresholds. By contrast, each kind of boundary strongly masks targets of the same kind. Our data is consistent with the possibility that luminance texture boundaries may be segmented using different mechanisms than those used to segment luminance step boundaries. At the same time, our work also suggests that LTB segmentation is subject to influences from LSBs. We suggest that the relative robustness of LTB segmentation to interference from LSBs may serve the ecologically important role of providing robustness to changes in luminance caused by cast shadows, and we propose future experimental work to investigate this hypothesis.

INTRODUCTION

An important intermediate step in visual processing is segmenting the image into distinct surfaces for purposes of scene analysis and identifying behaviorally relevant objects. One of the main cues available to visual systems for segmenting images are differences in luminance at the boundaries between two surfaces (**Mely, Kim, McGill, Guo, & Serre, 2016; DiMattina, Fox, & Lewicki, 2012; Hansen & Gegenfurtner, 2009; Martin, Fowlkes, & Malik, 2004**). In the boundary shown on the right of **Fig. 1a**, the luminance is constant within each surface, and there is a sharp change in luminance at the boundary, a situation which we refer to as a *luminance step boundary* (LSB). One of the consequences of this sharp change at the boundary will be that the boundary can be detected by operators defined at small spatial scales (**Elder & Sachs, 2004; Elder & Zucker, 1998; Marr, 1982**). However, in the boundary shown on the left of **Fig. 1a**, the luminance level varies greatly within each surface as well as between the two surfaces. Therefore, detecting the luminance difference between the surfaces requires integrating broadly over each surface, and there is no clear and obvious change in luminance at the boundary. We refer to this second situation as a *luminance texture boundary* (LTB), since the luminance cue is defined by the different relative proportion of dark and light regions inside each texture, and is only clearly visible when integrating over a large spatial scale.

Previous work in our laboratory on luminance boundary segmentation has suggested the possibility that different underlying mechanisms may sub-serve LTB and LSB segmentation (**DiMattina & Baker, 2020**). However, in that study masking was only considered in a paradigm at which both stimuli were presented at segmentation threshold. In this study, we further investigated the interactions between the two luminance cues using a supra-threshold masking paradigm in which observers segmented boundaries defined by one cue while ignoring a boundary

defined by the other **(Saarela & Landy, 2012**). We find that observers can quite successfully ignore a masking LSB when segmenting LTB targets, and vice-versa. However, observers were much more impaired when segmenting target boundaries in the presence of maskers of the same kind. Although we observed fairly weak masking of LTB targets by LSB maskers, we found that these effects are dependent on the relative congruency and phase of each kind of boundary, suggesting some degree of interaction between the two cues. These results strongly speak to the possibility that different (yet weakly interacting) mechanisms may be used for processing each kind of boundary. Finally, we propose possible models of the underlying segmentation mechanisms, and suggest novel directions for future research.

METHODS

Stimuli and Task

Stimuli

Luminance texture boundary (LTB) stimuli were created by placing different proportions of black (B) and white (W) micro-patterns on opposite halves of a circular disc. The visibility of the boundary was determined by the relative proportions (π_U) of white and black micro-patterns on each side of the boundary which are not balanced by a micro-pattern on the opposite side having the opposite polarity. The proportion of unbalanced patterns π_U can range from 0 (no boundary) to 1 (opposite colors on opposite sides). Examples of these stimuli are shown in **Fig. 1b**.

The LTB stimuli were 256x256 pixels and subtended 4 deg. visual angle (dva.), with 32 eight pixel Gaussian (σ = 2 pixels) micro-patterns on each side of the boundary. Maximum micro-pattern amplitude A was set to +/- 0.1, 0.2, or 0.25 (W/B) dimensionless luminance units with respect to the neutral gray mid-point (0.5), with Michealson contrast given by $c_M = 2A$. For all levels of A, the micro-patterns were clearly visible, as the lowest level (0.1) is roughly 3-4 times LTB contrast detection threshold. By design, stimuli had no luminance difference across the diagonal perpendicular to the boundary, and stimulus phase was set to either 0 or 180 degrees (left/right side brighter).

Luminance step boundaries (LSB) like those shown in **Fig. 1b** were created by multiplying an obliquely oriented step edge by a cosine-tapered circular disc. LSB stimuli were also 256 x 256 pixels and scaled to subtend 4 dva. The detectability of this edge was varied by manipulating its Michealson contrast c_M, and again the envelope phase was randomized.

Observers performed a 2AFC segmentation task identifying the orientation of a boundary (LTB or LSB) as either right-oblique (+45 deg. with respect to vertical, **Fig. 1b**) or left-oblique (-

45 deg. w.r.t. vertical). Boundary visibility was adjusted for each type of stimulus (LSB, LTB) using a 1-up, 2-down staircase procedure, which focused trials at stimulus levels leading to 70.71% correct performance. Initial experiments were conducted to obtain thresholds for each boundary in its natural units (LTB: π_U, LSB: c_M). For purposes of data analysis, both kinds of boundary can be expressed in JND units, as well as (dimensionless) units of luminance difference across the diagonal.

Observers

Author CJD and three naïve undergraduate student researchers (KNB, ERM, MXD) who were experienced with the segmentation tasks served as observers in these experiments. All observers gave informed consent, and all experimental procedures were approved by the FGCU IRB (Protocol 2014-01), in accordance with the Declaration of Helsinki.

Visual Displays

Stimuli were presented in a dark room on a 1920x1080, 120 Hz gamma-corrected Display++ LCD Monitor (Cambridge Research Systems LTD®) with mid-point luminance of 100 cd/m^2. This monitor was driven by an NVIDA GeForce® GTX-645 graphics card, and experiments were controlled by a Dell Optiplex® 9020 running custom-authored software written in MATLAB® making use of Psychtoolbox-3 routines (**Brainard, 1997; Pelli, 1997**). Observers were situated 133 cm from the monitor using a HeadSpot® chin-rest, so that the 256x256 stimuli subtended approximately 4 deg. of visual angle.

Experimental Protocols

<u>Experiment 1: Masking luminance texture boundaries with luminance step boundaries</u>

In order to investigate the effects of luminance step boundaries (LSBs) on the segmentation of luminance texture boundaries (LTBs), four observers (CJD, ERM, KNB, MXD) segmented LTBs

in the presence of masking LSBs (**Fig. 1c**, top row). Masking luminance steps were presented at multiples of LSB segmentation threshold (1, 2, 4, 8x JND). For the luminance steps, maximum micro-pattern amplitude A was set to 0.1 or 0.2 (MXD only did 0.1), and segmentation thresholds were obtained by varying the proportion of unbalanced micro-patterns π_U using a staircase procedure for 240 trials. The design was balanced so that for an equal number of trials the target LTB and masking LSB had congruent (120 trials) and incongruent orientations (120 trials). Within the set of 120 congruently oriented trials, an equal number of trials had the two stimuli phase-aligned and opposite phase.

Experiment 2: Masking luminance step boundaries with luminance step boundaries

For purposes of comparison, two observers in **Experiment 1** (CJD, KNB) also completed a second experiment (**Experiment 2**) in which they segmented luminance step boundaries in the presence of a masking luminance step boundary (**Fig. 1c**, second row). Masking boundaries were presented at multiples of LSB segmentation threshold (1, 2, 4x JND), and the relative orientations and phases of target and masker were balanced as in **Experiment 1**.

Experiment 3: Masking luminance step boundaries with luminance texture boundaries

Three observers (CJD, KNB, MXD) also segmented luminance steps in the presence of luminance texture boundaries which served as maskers (**Fig. 1c**, third row). LTB stimuli were presented at $A = 0.1$ and the proportion of unbalanced micro-patterns π_U was set at 0, 1, 2, and 4x JND. Observers were instructed to segment the steps while ignoring the masking texture boundaries. Relative orientations and phases of target and masker were balanced as in **Experiment 1**.

Experiment 4: Masking luminance texture boundaries with luminance textures

Observers CJD and MXD completed a final set of trials in which they segmented a luminance texture boundary in the presence of a masking luminance texture which was added to the target (**Fig. 1c**, bottom row). Both target and masking luminance texture boundaries were presented at $A = 0.1$, and the masker was presented at multiples of its segmentation threshold for each observer (0, 1, 2x JND). Relative orientations and phases of target and masker were balanced as in **Experiment 1**.

Data Analysis

Psychometric function fitting

Data was fit using a signal-detection theory (SDT) psychometric model (**Kingdom & Prins, 2016**), where the proportion correct (P_C) for a single-interval classification task is given by

$$P_C = \frac{\lambda}{2} + (1-\lambda)\Phi\left(\frac{d'}{2}\right), \quad (1)$$

$$d' = [gx]^{\tau}, \quad (2)$$

where d' is the separation of two (unit standard deviation) Gaussian distributions representing each category, with stimulus intensity x, and free parameters of gain g, transducer exponent τ and lapse rate λ. The SDT model was fit to psychophysical data using MATLAB® routines from the Palemedes Toolbox (http://www.palamedestoolbox.org/), as described in **Prins & Kingdom (2019)**. Note that one can also equivalently interpret (1) as a model in which the outputs of two mechanisms (right and left) are subtracted to form a decision variable which is then compared to zero, assuming that the distributions describing the responses of each mechanism have a standard deviation of $1/\sqrt{2}$.

Bootstrapping psychometric functions

Bootstrapping was employed to plot non-parametric 68% and/or 95% confidence intervals for the psychometric function thresholds. For bootstrapping analyses, N = 200 simulated datasets were created as follows: For each stimulus level with n_i presentations and c_i experimentally observed correct responses (proportion of correct responses $p_i = c_i/n_i$), we sampled from a binomial distribution having n_i trials with probability p_i to create a simulated number of correct responses for that stimulus level. We fit our models to each of these simulated datasets, and obtained distributions of the psychometric function parameters, as well as the stimulus levels corresponding to JND (75% correct) performance.

Generic linear masking model

In order to compare the observed threshold elevations to those we might expect when the masker and target are processed by identical mechanisms, we consider the following generic model. Assume that a decision variable $u = u_R - u_L$ is obtained by subtracting the outputs of a right-oblique (R) mechanism and a left-oblique (L) mechanism. Assume that the R mechanism has mean response $\mu_R(x) = gx$ for R stimulus (0 otherwise) and stimulus-independent Gaussian noise ($\sigma = 1/\sqrt{2}$), and assume an identical L mechanism. The decision variable $u = u_R - u_L$ is distributed with a mean $\mu_R - \mu_L$ and unit variance. Assume without loss of generality that the target is right-oblique, and assume zero lapse rate. In the absence of a mask, the probability of a correct response P_C is $P(u > 0)$, given by

$$P_C = \Phi\left(\frac{\mu_R - \mu_L}{2}\right) = \Phi\left(\frac{gx}{2}\right), \tag{3}$$

and JND performance level $0 \leq J \leq 1$ is obtained with stimulus level $x_J = \frac{2}{g}\Phi^{-1}(J)$. Now, assume we have a left-oblique mask set at level nx_J, so that $\mu_L = gnx_J$. For a right-oblique target,

the mean output of the right-oblique mechanism is given by $\mu_R = gx$, and from (3) we obtain JND performance level J for $x = (n + 1)x_J$.

Although this model provides a useful generic prediction about how maskers processed by identical mechanisms as target stimuli should effect segmentation, it is important to note that stimulus transduction is often nonlinear (**Solomon, 2009; Morgan, Chubb, & Solomon, 2009; Kingdom & Prins, 2016**). Furthermore, although most masking studies assume fixed internal noise levels that do not depend on masker amplitude (e.g., **Legge & Foley, 1980**), this assumption remains a point of debate (**Kingdom, 2016**).

RESULTS

Effects of LSB maskers on LTB targets

In order to examine the effects of luminance step boundary (LSB) maskers on luminance texture boundary (LTB) segmentation thresholds, all observers performed an LTB segmentation task (**Experiment 1**) in the presence of supra-threshold masking LSBs, with contrasts set at various multiples of LSB segmentation JND (1, 2, 4, 8x). As shown in **Fig. 2a**, in the presence of the LSB maskers, we observed modest elevations of LTB detection threshold in both natural units (proportion unbalanced micro-patterns π_U) and JND units for both values of LTB Michaelson contrast c_M (0.2: green, 0.4: blue). To get a visual intuition for the degree of threshold elevation, at low contrast the worst performing observer (CJD) went from a threshold of about π_U= 0.25 to about π_U = 0.5, corresponding to the difference between the LTB stimuli in rows 2 and 3 of **Fig. 1a**. We see in **Fig. 2a** that observer KNB exhibited almost no increase in thresholds in **Experiment 1**, with ERM and MXD exhibiting intermediate results. Averaged results for observers completing all conditions are given in **Fig. 2b**. The predictions of a generic linear masking model (**Methods**) is shown by the dashed lines in **Fig. 2a, b** (left columns), and we see that the observed threshold elevations fall well below these predictions, consistent with the possibility of different mechanisms being used to segment LTB and LSB stimuli.

Two-way ANOVAs on bootstrapped thresholds yielded nearly identical results whether thresholds were analyzed in JND units or natural units. Therefore, we present all ANOVA results in JND units, which permits comparisons between LTB and LSB stimuli. In **Experiment 1**, ANOVA revealed for the observers completing all conditions a highly significant ($p < 0.001$ in all cases) effect of the LSB masker level (KNB: $F_{4,1990} = 1572.8$, $\eta^2 = 0.665$; ERM: $F_{4,1990} = 2356.5$, $\eta^2 = 0.401$; CJD: $F_{4,1990} = 6509.22$, $\eta^2 = 0.893$). Similarly, we observed a smaller yet highly

significant effect ($p < 0.001$) of the LTB target contrast (KNB: $F_{1,1990} = 523.2$, $\eta^2 = 0.055$; ERM: $F_{1,1990} = 8404.4$, $\eta^2 = 0.357$; CJD: $F_{1,1990} = 784.76$, $\eta^2 = 0.027$), as well as a highly significant ($p < 0.001$) interaction (KNB: $F_{4,1990} = 164.3$, $\eta^2 = 0.069$; ERM: $F_{4,1990} = 927.6$, $\eta^2 = 0.158$; CJD: $F_{4,1990} = 83.11$, $\eta^2 = 0.011$). This quantitative analysis confirms what we see qualitatively in **Fig 2**: masking was stronger for higher masker levels, and the low-contrast LTB (green symbols) was masked more than the higher contrast LTB (blue symbols).

For purposes of comparison with **Experiment 1**, observers CJD and KNB performed a control experiment (**Experiment 2**) in which they segmented a luminance step boundary (LSB) in the presence of the same LSB maskers used in **Experiment 1**. The basic idea of **Experiment 2** is to consider a case in which the target and the masker will necessarily activate the same mechanisms. We see in **Fig. 3** that segmentation thresholds in JND units were drastically elevated for both observers by the masking LSBs (**Fig. 3**, black symbols). This stands in stark contrast with the relatively modest increases in LTB segmentation thresholds induced by these same maskers in **Experiment 1** (**Fig. 3**, blue and green symbols). Note that here the threshold elevations fall above the theoretical predictions of the simple linear transducer model (black dashed lines), consistent with the well-known fact that contrast detection thresholds increase with pedestal contrast for supra-threshold maskers. A 2-way ANOVA revealed a highly significant difference for the two targets (KNB: $F_{1,1194} = 7552$, $\eta^2 = 0.503$, $p < 0.001$; CJD: $F_{1,1194} = 8574$, $\eta^2 = 0.434$, $p < 0.001$), masker level (KNB: $F_{2,1194} = 1795$, $\eta^2 = 0.239$, $p < 0.001$; CJD: $F_{2,1194} = 3179$, $\eta^2 = 0.321$, $p < 0.001$) and interaction (KNB: $F_{2,1194} = 1336$, $\eta^2 = 0.178$, $p < 0.001$; CJD: $F_{2,1194} = 1826$, $\eta^2 = 0.185$, $p < 0.001$). Taking **Experiments 1** and **2** as a whole, the drastically different effects of the same LSB maskers on different luminance boundary targets (LTB, LSB) is certainly consistent with the

hypothesis that the underlying mechanisms responsible for segmenting these boundaries may be different.

Effects of relative orientation and phase

Although the increases in threshold observed in **Experiment 1** were modest, breaking down trials by the relative orientations and phases of the LTB target and LSB masker revealed some degree of interaction between the two luminance cues. We see in **Fig. 4** that segmentation thresholds were lowest when the LSB masker and LTB target had congruent orientations and were phase-aligned (**con-0**, cyan symbols), were highest for congruent orientations which were opposite-phase (**con-180**, magenta symbols), and intermediate for incongruent orientations (**inc**, red symbols). Plots on **Fig. 4a**, **b** are shown in natural units (π_U), and those in **Fig. 4c**, **d** are shown in JND units. Marginal mean thresholds in JND units for each observer are shown in **Table 1**.

	KNB	**ERM**	**CJD**
inc	1.117	1.138	2.053
con-0	1.026	0.892	1.630
con-180	1.374	1.446	2.187

Table 1: Marginal mean JNDs for congruency/phase levels

We performed a 3-way ANOVA on the bootstrapped thresholds for observers completing all conditions. A significant effect of congruency/phase condition (**inc**, **con-0**, **con-180**) was demonstrated for all observers (KNB: $F_{2,4776} = 940.45$, $\eta^2 = 0.149$, $p < 0.001$; ERM: $F_{2,4776} = 3404.10$, $\eta^2 = 0.242$, $p < 0.001$; CJD: $F_{2,4776} = 1215.153$, $\eta^2 = 0.130$, $p < 0.001$). Post-hoc pairwise *t*-tests comparing performance for pairs of congruency/phase conditions demonstrated significant differences ($p < 0.001$, Tukey HSD) between all conditions for all observers. Therefore, we conclude that although the elevations in LTB segmentation threshold caused by LSB maskers are modest, there are real differences in thresholds depending on the relative phase of the target and

masking cues, suggesting that the mechanisms used for LTB segmentation are not entirely immune to influence from LSB maskers.

Effects of LTB maskers on LSB targets

Three observers (CJD, KNB, MXD) performed an experiment (**Experiment 3**) which serves as the converse of **Experiment 1**, with observers segmenting luminance step boundaries (LSBs) in the presence of (low-contrast) masking luminance textures (LTBs). The goal was to see if LTBs interfered with LSB segmentation to the same degree as LSBs interfered with LTBs, as well as if there were similar interactions of phase and congruency conditions seen in **Experiment 1**. We see in **Fig. 5a** that the increases in LSB segmentation thresholds were fairly modest in the presence of LTB maskers (red symbols). This was similar to the finding of **Experiment 1,** which found comparably modest increases to LTB segmentation thresholds in the presence of LSB masker (**Fig. 2**). The results for **Experiment 1** (**Fig. 2**) for the low-contrast case (0.2) are plotted in **Fig. 5b** for purposes of comparison (green symbols). We see that at least qualitatively there are very similar levels of masking regardless of which kind of boundary is the target and the mask. Performing a two-way ANOVA on the data in **Fig. 5b** demonstrated that although both factors (and their interaction) exhibited significant effects on thresholds ($p < 0.001$), there was a much smaller effect size of target-masker pairing (LTB/LSB vs. LSB/LTB target/masker) than masker level (KNB: $\eta^2_{lev} = 0.582$, $\eta^2_{pair} = 0.017$; MXD: $\eta^2_{lev} = 0.672$, $\eta^2_{pair} = 0.162$; CJD: $\eta^2_{lev} = 0.851$, $\eta^2_{pair} = 0.016$). We see in **Fig. 5b** that for each individual observer (and their average) that in JND units, an LSB masker (green) affects LTB segmentation similarly to how an LTB masker affects LSB segmentation (red).

In contrast to **Experiment 1**, we did not find consistently better LSB segmentation performance when the LTB masker was congruent (**con-0**) and phase-aligned than when it was

congruent and opposite-phase (**con-180**). In fact, in contrast to **Experiment 1** (**Table 1**), for two of the three observers (KNB, MXD) the marginal mean thresholds (JND units) were higher in the **con-0** case than **con-180** case (KNB: **con-0** = 1.242, **con-180** = 1.196, t_{1598} = 2.402, p = 0.043; MXD: **con-0** = 1.358, **con-180** = 1.180, t_{1598} = 6.871, p < 0.001), although the overall effect of phase/congruency was quite small for these observers (KNB: η^2 = 0.003; MXD: η^2 = 0.018). Only for author CJD were there effects ($F_{2,2388}$ = 502.1, p < 0.001, η^2 = 0.167) of phase/congruency consistent with those seen in **Experiment 1** (**con-0**: 1.410, **con-180**: 2.344, **inc**: 1.869; all pairwise comparisons p < 0.001).

Finally, observers CJD and MXD performed the LTB segmentation task in the presence of a masking LTB which was added to the target, at 3 levels of masker level (0, 1, 2x JND), with 0 JND corresponding to an LTB masker with $\pi_U = 0$. **Fig. 6** shows the segmentation thresholds for LTB targets (magenta symbols) as well as LSB targets (red symbols). We see that LTB maskers severely impair the detection of LTB targets (magenta symbols), to an even greater extent than would be predicted by the generic linear masking model (black dashed lines). By contrast these same maskers exhibit little effect on LSB stimulus segmentation (red lines). Two-way ANOVA revealed significant effects (p <0.001) of target type (CJD: $F_{1,1194}$ = 17087.9, η^2 = 0.758; MXD: $F_{1,1194}$ = 51551.4, η^2 = 0.916), masker JND (CJD: $F_{2,1194}$ = 1602.5, η^2 = 0.142; MXD: $F_{2,1194}$ = 1028.9, η^2 = 0.037) and their interaction (CJD: $F_{2,1194}$ =527.6, η^2 = 0.047; MXD: $F_{2,1194}$ = 745.3, η^2 = 0.026), with the largest effect sizes for target type.

<u>Analysis in terms of absolute luminance differences</u>

The previous analyses put the two stimuli on equal footing by formulating thresholds in units of multiples of JND. Although such a formulation in represents common practice in the larger vision science literature, another way which one can place these stimuli on equal footing is by expressing

their intensity in units of absolute luminance differences across the diagonal. **Fig. 7** shows the thresholds in **Experiments 1** and **2** for observers CJD, KNB. Here we plot the LSB masker and target (LTB and/or LSB) in units of absolute luminance difference (**Fig. 7a**: LTB target, **Fig. 7b:** LSB + LTB target). We see that when segmenting an LTB in the presence of a masking LSB, a far smaller luminance difference is required than predicted by a generic linear masking model (**Fig. 7a**, dashed lines) for observers to segment the LTB. In contrast, when segmenting an LSB in the presence of an LSB masker, thresholds are generally above the level of the masker predicted by the generic linear model. This analysis further supports the idea that different mechanisms may be responsible for segmenting each kind of boundary.

DISCUSSION

Overview

In natural images, multiple visual cues for boundary segmentation are available, including texture, color and luminance (**Mely et al., 2016; DiMattina et al., 2012; Martin et al., 2004**). In previous work (**DiMattina & Baker, 2021**), we introduced the distinction between luminance texture boundaries (LTBs) and luminance step boundaries (LSBs), and conducted a series of experiments suggesting that LTB and LSB stimuli may be segmented via different mechanisms. This earlier work only examined the robustness of LTB segmentation to interference from masking LSBs when the masker was presented at segmentation threshold. However, in natural vision we typically segment surfaces in the presence of interfering luminance cues arising from clearly visible shadows (**Mammasian, Knill, & Kersten, 1998; Kingdom, Beauce, & Hunter, 2004; Casati & Cavanaugh, 2019**). In the present study, we investigated the segmentation of luminance texture boundaries (LTBs) in the presence of supra-threshold LSBs, and also put these results into a larger context by considering all other possible combinations of masker and target (LTB/LSB, LSB/LSB, LTB/LTB) as well. We find that each kind of luminance boundary unsurprisingly masks boundaries of the same category, but quite interestingly exhibits relatively little effect on luminance boundaries of the other category. This strongly suggests that there may be multiple, distinct mechanisms which contribute to the processing of luminance boundary cues in early vision. Although the interference between boundary categories is relatively small, it is important to note that it is not zero. In fact, for the case of LTB segmentation in the presence of an interfering LSB masker, we observed strong effects of the relative phase and orientation of the target and masker in all observers (**Fig. 4**). This psychophysical observation may provide an important clue about underlying neural mechanisms.

Possible Mechanisms

Our psychophysical results from **Experiment 1** suggest that the mechanisms of LTB boundary segmentation must be resistant to influence from interfering LSB masker stimuli (**Fig. 2**), even when these maskers give rise to far greater luminance difference than the LTB target (**Fig. 7**). Therefore, we can rule out a simple luminance difference mechanism like that illustrated in **Fig. 8a**, as such a model would be highly susceptible to interference from masking LSBs. One possible model consistent with our data is shown in **Fig. 8b**. This model is comprised of two stages of filters: A set of localized first-stage center-surround filters which detect the individual black and white micropattterns, followed by a second stage of filtering which integrates broadly over the entire boundary. Such a model would be able to detect luminance texture boundaries with minimal interference from luminance steps. However, if the first-stage filters exhibit a non-zero DC response, there is the potential for the phase of a masking LSB having a congruent boundary orientation to influence segmentation thresholds, as we observed in our data (**Fig. 4**). However, this is by no means the only possible explanation for our observed interactions: It might also be the case that there are separate parallel mechanisms optimized for luminance textures and luminance steps, and the outputs of each mechanism are combined downstream to obtain the final perceptual decision (**Fig. 8c**). It remains for future work to develop experiments to distinguish between these two interesting possibilities.

Limitations and Future Directions

The present study making use of artificial luminance-defined texture boundaries is intended as a modest first step towards addressing the larger question of how luminance cues are processed to facilitate boundary segmentation. These stimuli provide the advantage that they are simple to generate and contain no textural cues other than luminance which can possibly influence

segmentation. However, the convenience of working with artificial stimuli comes at the cost that they may have limited utility for understanding natural vision, an issue long debated in neurophysiology (**Felsen & Dan, 2005; Rust & Movshon, 2005**). It is of interest for us in future work to develop algorithms for manipulating natural textures in order to create luminance differences across a boundary by manipulating the relative proportion of dark and light areas on opposite sides of the boundary. Segmentation of such stimuli could be compared to the segmentation of texture stimuli with luminance steps added, in order to compare the relative efficacy of each kind of cue for segmentation. By controlling for the absolute luminance difference (Fig. 7) one can directly test the hypothesis that the visual system is more sensitive to luminance textures than luminance steps, since steps may arise from case shadows.

Natural texture boundaries will not only contain differences in luminance, but also differences in various second-order texture cues like orientation (**Wolfson & Landy, 1998**), micro-pattern density (**Zavitz & Baker, 2014**), and contrast (**Dakin & Mareschal, 2000**; **DiMattina & Baker, 2019**). It is of interest for future work to better understand how luminance cues (step and boundary) interact with these various second-order texture cues for boundary segmentation. This can be accomplished using various sub-threshold summation paradigms and fitting quantitative models of cue combination to the data (e.g., **Motoyoshi & Nishida, 2004; Kingdom et al. 2015**). Previous psychophysical work studying the interaction of first and second-order cues has focused on detection tasks, and these results have suggested separate mechanisms for processing first- and second-order cues (**Schofield & Georgeson, 1999; Allard & Faubert, 2007**). By contrast, neurophysiological investigations have suggested the existence of "form-cue invariant" responses which respond to boundaries defined by either first or second-order cues (**Li et al, 2014**), and even demonstrated nonlinear interactions between these cues (**Hutchinson,**

Ledgeway, & Baker, 2016). To our knowledge, psychophysical work has yet to systematically investigate the combination of first- and second- order cues specifically for segmentation in a systematic manner using standard summation paradigms. Of particular interest is comparing the interactions between first-order and second-order information in two cases: (1) Where the first-order cue is defined by texture (LTB), as might be the case for two different surfaces, and (2) The first-order cue is a luminance step (LSB), which can possibly be caused by a shadow. One reasonable hypothesis is that we may observe a greater degree of summation between first- and second-order cues in case (1) than in case (2), since changes in texture micro-pattern properties provide stronger evidence for a surface boundary. This intriguing possibility remains to be investigated in future experimental work.

REFERENCES

Allard, R., & Faubert, J. (2007). Double dissociation between first-and second-order processing. *Vision Research*, *47*(9), 1129-1141.

Brainard, D. H. (1997). The psychophysics toolbox. *Spatial Vision*, *10*(4), 433-436.

Casati, R., & Cavanagh, P. (2019). *The Visual World of Shadows*. MIT Press.

Dakin, S. C., & Mareschal, I. (2000). Sensitivity to contrast modulation depends on carrier spatial frequency and orientation. *Vision Research*, *40*(3), 311-329.

DiMattina, C., & Baker Jr., C. L. (2019). Modeling second-order boundary perception: A machine learning approach. *PLoS Computational Biology*, *15*(3), e1006829.

DiMattina, C., & Baker Jr., C.L. (2020). Segmenting surface boundaries using luminance cues: Underlying mechanisms. *bioRxiv.org.* doi: *https://doi.org/10.1101/2020.06.27.175505*

DiMattina, C., Fox, S. A., & Lewicki, M. S. (2012). Detecting natural occlusion boundaries using local cues. *Journal of vision*, *12*(13), 15-15.

Elder, J. H., & Sachs, A. J. (2004). Psychophysical receptive fields of edge detection mechanisms. *Vision Research*, *44*(8), 795-813.

Elder, J. H., & Zucker, S. W. (1998). Local scale control for edge detection and blur estimation. *IEEE Transactions on pattern analysis and machine intelligence*, *20*(7), 699-716.

Felsen, G., & Dan, Y. (2005). A natural approach to studying vision. *Nature neuroscience*, *8*(12), 1643-1646.

Hansen, T., & Gegenfurtner, K. R. (2009). Independence of color and luminance edges in natural scenes. *Visual neuroscience*, *26*(1), 35.

Hutchinson, C. V., Ledgeway, T., & Baker, C. L. (2016). Phase-dependent interactions in visual cortex to combinations of first-and second-order stimuli. *Journal of Neuroscience*, *36*(49), 12328-12337.

Kingdom, F.A.A., Baldwin, A. S., & Schmidtmann, G. (2015). Modeling probability and additive summation for detection across multiple mechanisms under the assumptions of signal detection theory. *Journal of Vision*, *15*(5), 1-1.

Kingdom, F. A. (2016). Fixed versus variable internal noise in contrast transduction: The significance of Whittle's data. *Vision research*, *128*, 1-5.

Kingdom, F. A., Beauce, C., & Hunter, L. (2004). Colour vision brings clarity to shadows. *Perception*, *33*(8), 907-914.

Kingdom, F.A.A., & Prins, N. (2016). *Psychophysics: a practical introduction*. Academic Press.

Legge, G. E., & Foley, J. M. (1980). Contrast masking in human vision. *Josa*, *70*(12), 1458-1471.

Mamassian, P., Knill, D. C., & Kersten, D. (1998). The perception of cast shadows. *Trends in cognitive sciences*, *2*(8), 288-295.

Marr, D. (1982). Vision: A computational investigation into the human representation and processing of visual information. Henry Holt and Co. Inc., *New York, NY*.

Martin, D. R., Fowlkes, C. C., & Malik, J. (2004). Learning to detect natural image boundaries using local brightness, color, and texture cues. *IEEE Transactions on Pattern Analysis and Machine Intelligence*, *26*(5), 530-549.

Mély, D. A., Kim, J., McGill, M., Guo, Y., & Serre, T. (2016). A systematic comparison between visual cues for boundary detection. *Vision research*, *120*, 93-107.

Morgan, M., Chubb, C., & Solomon, J. A. (2008). A 'dipper'function for texture discrimination based on orientation variance. *Journal of vision*, *8*(11), 9-9.

Motoyoshi, I., & Nishida, S. Y. (2004). Cross-orientation summation in texture segregation. *Vision Research*, *44*(22), 2567-2576.

Pelli, D. G. (1997). The VideoToolbox software for visual psychophysics: Transforming numbers into movies. *Spatial vision*, *10*(4), 437-442.

Prins, N., & Kingdom, F.A.A. (2018). Applying the model-comparison approach to test specific research hypotheses in psychophysical research using the Palamedes toolbox. *Frontiers in psychology*, *9*, 1250.

Rust, N. C., & Movshon, J. A. (2005). In praise of artifice. *Nature neuroscience*, *8*(12), 1647-1650.

Saarela, T. P., & Landy, M. S. (2012). Combination of texture and color cues in visual segmentation. *Vision Research*, *58*, 59-67.

Schofield, A. J., & Georgeson, M. A. (1999). Sensitivity to modulations of luminance and contrast in visual white noise: Separate mechanisms with similar behaviour. *Vision Research*, *39*(16), 2697-2716.

Solomon, J. A. (2009). The history of dipper functions. *Attention, Perception, & Psychophysics*, *71*(3), 435-443.

Wolfson, S. S., & Landy, M. S. (1998). Examining edge-and region-based texture analysis mechanisms. *Vision Research*, *38*(3), 439-446.

Zavitz, E., & Baker, C. L. (2014). Higher order image structure enables boundary segmentation in the absence of luminance or contrast cues. *Journal of vision*, *14*(4), 14-14.

FIGURE CAPTIONS

Figure 1: Stimuli and experimental conditions

(**a**) Examples of luminance texture boundaries (LTBs, *right*) and luminance step boundaries (LSBs, *left*). By construction, the luminance step boundary has the exact same luminance difference as the luminance texture boundary.

(**b**) Luminance texture boundary (LTB) stimuli with a right-oblique boundary orientation and varying levels of the parameter π_U which determines boundary visibility. The parameter specifies the proportion of micro-patterns on each side which are not balanced by a micro-pattern of opposite polarity on the opposite side.

(**c**) Schematic depiction of the target stimuli and masking stimuli for each experiment. Observers were instructed to determine the orientation of the target stimulus boundary, while ignoring the masking stimulus.

Figure 2: Experiment 1 results

(**a**) LTB segmentation thresholds as a function of masking luminance step boundary (LSB) level for two levels of LTB contrast c_M (0.2: green symbols, 0.4: blue symbols). Symbols indicate medians, and error-bars indicate 68% (non-parametric) confidence intervals obtained from 200 bootstrapped fits of the psychometric function. Thresholds are plotted in both natural units (left column), as well as units of LTB segmentation JND (right column). The dashed black line in the right column plots indicates the segmentation thresholds predicted by a generic linear masking model (see **Methods** for details).

(**b**) Same as (a), averaged across observers who completed all conditions of **Experiment 1**.

Figure 3: Comparison of Experiment 1 and Experiment 2 results

Segmentation thresholds in JND units for a luminance step boundary (LSB) target in the presence of an LSB masker (black symbols, vertical lines denote 68% confidence intervals) for both observers completing **Experiment 2**, as well as their averaged results (right panel). We see that when the target and masker are both LSB stimuli, that segmentation thresholds increase linearly with LSB masker level, exceeding the predictions of a generic linear masking model (black dashed lines). By comparison, LTB segmentation thresholds (JND units) increase much more slowly (blue and green symbols, confidence intervals not shown) with LSB masker level.

Figure 4: Effects of boundary orientation congruency and relative phase

(**a**) Luminance texture boundary (LTB) segmentation thresholds from **Experiment 1** in natural units (π_U), decomposed by the relative boundary orientation (congruent/incongruent) and phase-alignment (same/opposite) of target and masker stimuli. Red symbols indicate segmentation thresholds when LTB target and LSB masker had incongruent orientations (**inc**). For stimuli with congruent orientations we plot segmentation thresholds for same-phase (**con-0,** cyan symbols) and opposite-phase (**con-180,** magenta symbols). Error bars indicate 68% bootstrapped confidence intervals.

(**b**) Same as (a), but averaged across observers.

(**c**) Same as (a), but plotted in JND units.

(**d**) Same as (c), but averaged across observers.

Figure 5: Experiment 3 results

(**a**) Luminance step boundary (LSB) segmentation thresholds in JND units (red symbols) as a function of LTB masker level obtained in **Experiment 3**. Error bars indicate 95% confidence intervals.

(**b**) Comparison of segmentation thresholds (JND units) for both combinations of target-masker stimulus type (**Experiment 1**: LTB target, LSB mask, green symbols; **Experiment 3**: LSB target, LTB mask, red symbols). We see very similar degrees of interference for both combinations of target-masker stimulus type.

Figure 6: Experiment 4 results

Segmentation thresholds for luminance texture boundary (LTB) stimuli in the presence of LTB maskers (magenta symbols), and thresholds for luminance step boundary (LSB) stimuli in the presence of these same LTB maskers (red symbols).

Figure 7: Experiment 1 and 2 in units of absolute luminance difference

(**a**) Results of **Experiment 1** with LSB masker luminance and LTB target luminance plotted in the same units (blue and green symbols), together with predictions of linear masker model (dashed lines).

(**b**) Results of **Experiment 2** plotted in units of absolute luminance difference (black symbols), together with linear masker model prediction (dashed lines) and results of **Experiment 1** (blue and green symbols).

Figure 8: Hypothetical models of luminance boundary segmentation

(**a**) Model with two large-scale filters which compute luminance differences across each diagonal.

(**b**) Model with two stages of filtering. A set of first-stage filters defined on a small spatial scale detects the light and dark micro-patterns, and second stage filters defined on the scale of the entire image looks for differences across the diagonal in the outputs of the second stage filters.

(**c**) Third model which combines outputs from a single-stage and two-stage models shown in (a) and (b).

FIGURE 1

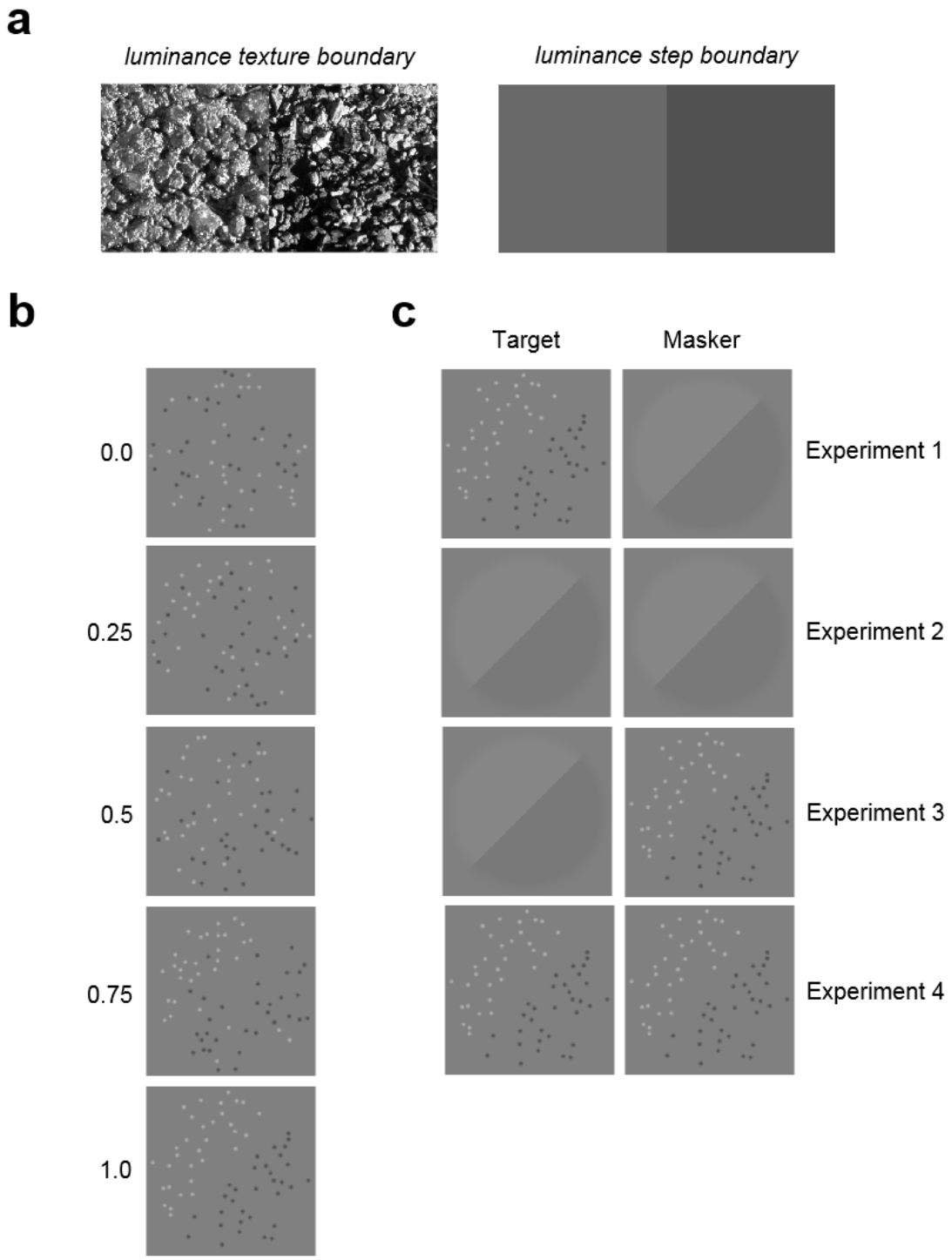
a
luminance texture boundary
luminance step boundary
b
0.0
0.25
0.5
0.75
1.0
c
Target
Masker
Experiment 1
Experiment 2
Experiment 3
Experiment 4

FIGURE 2

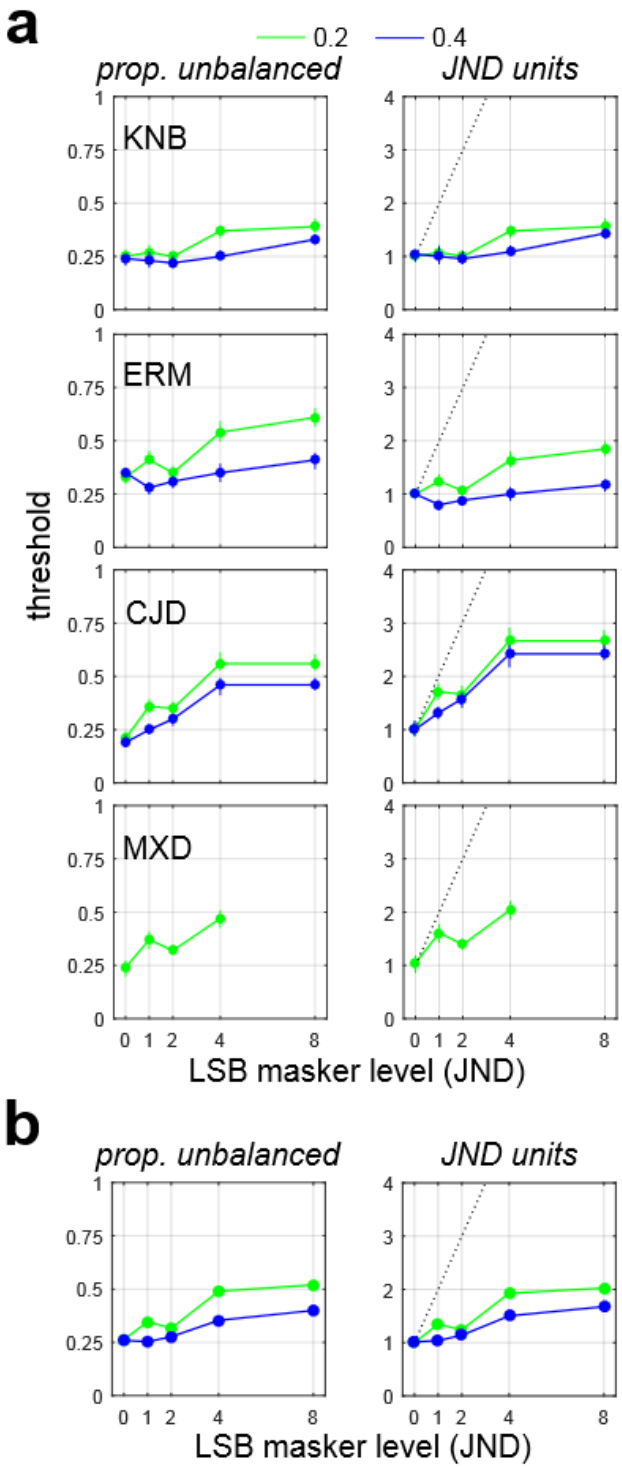
a
0.2
0.4
prop. unbalanced
JND units
KNB
ERM
CJD
MXD
threshold
LSB masker level (JND)
b
prop. unbalanced
JND units
LSB masker level (JND)

FIGURE 3

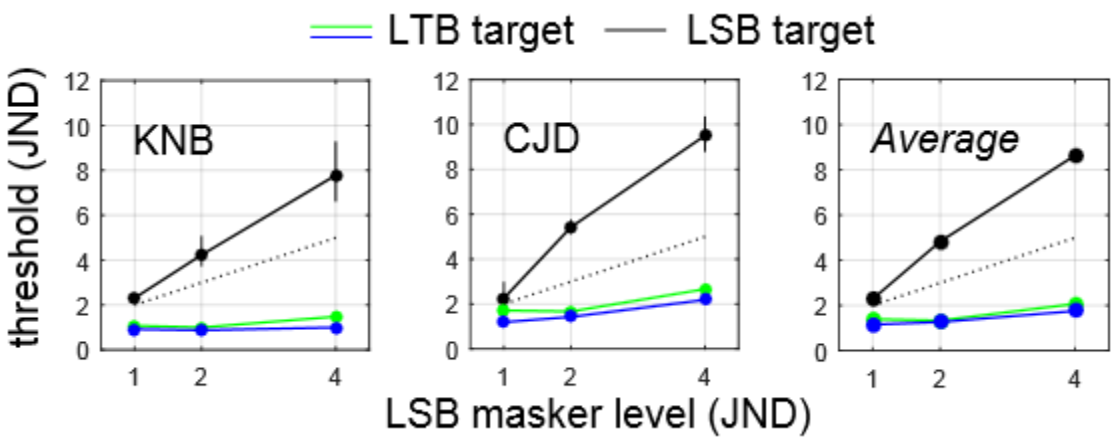
LTB target
LSB target
threshold (JND)
KNB
CJD
Average
0
2
4
6
8
10
12
1
2
4
LSB masker level (JND)

FIGURE 4

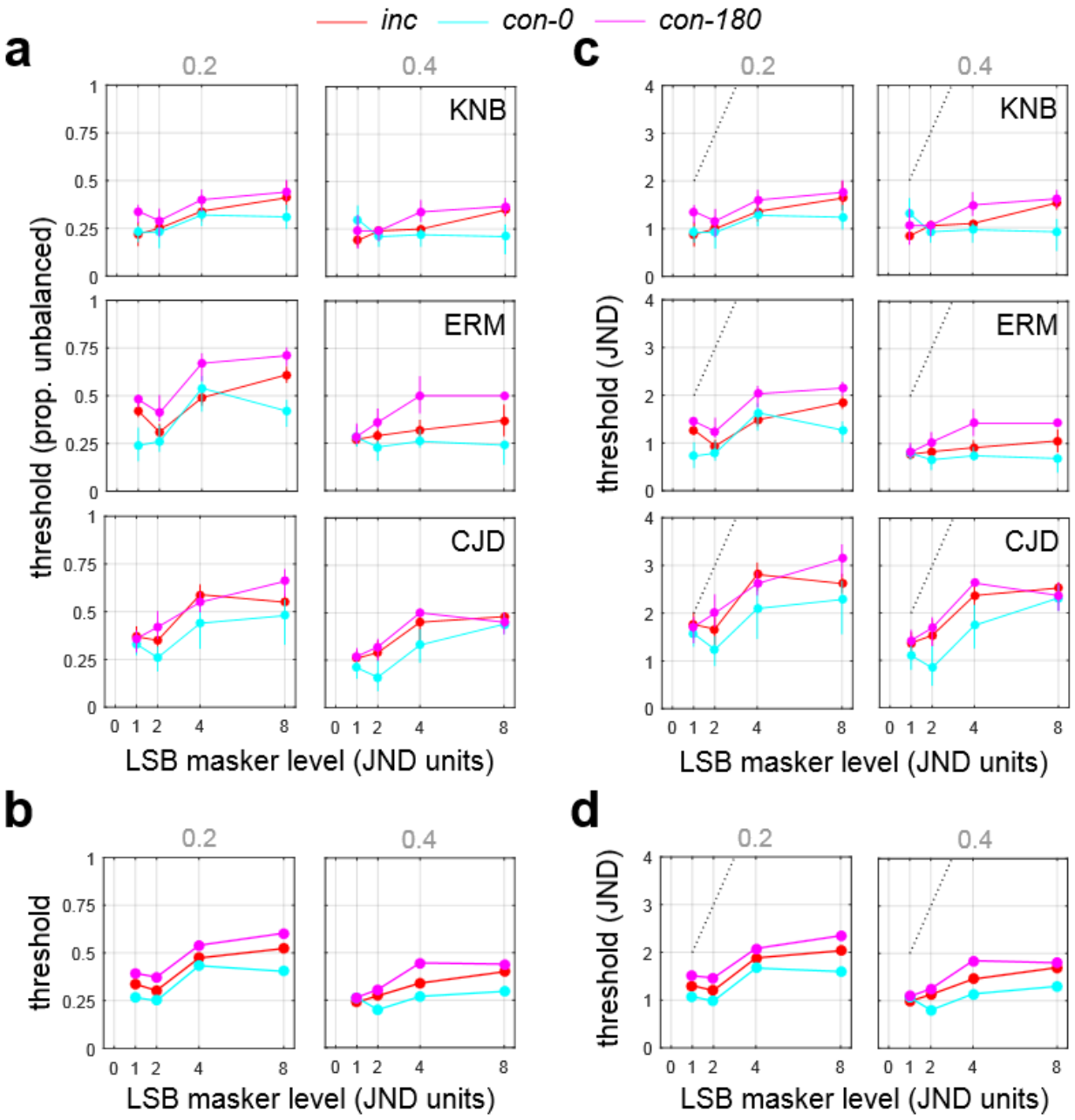
inc
con-0
con-180
a
b
c
d
0.2
0.4
KNB
ERM
CJD
threshold (prop. unbalanced)
threshold (JND)
threshold
LSB masker level (JND units)

FIGURE 5

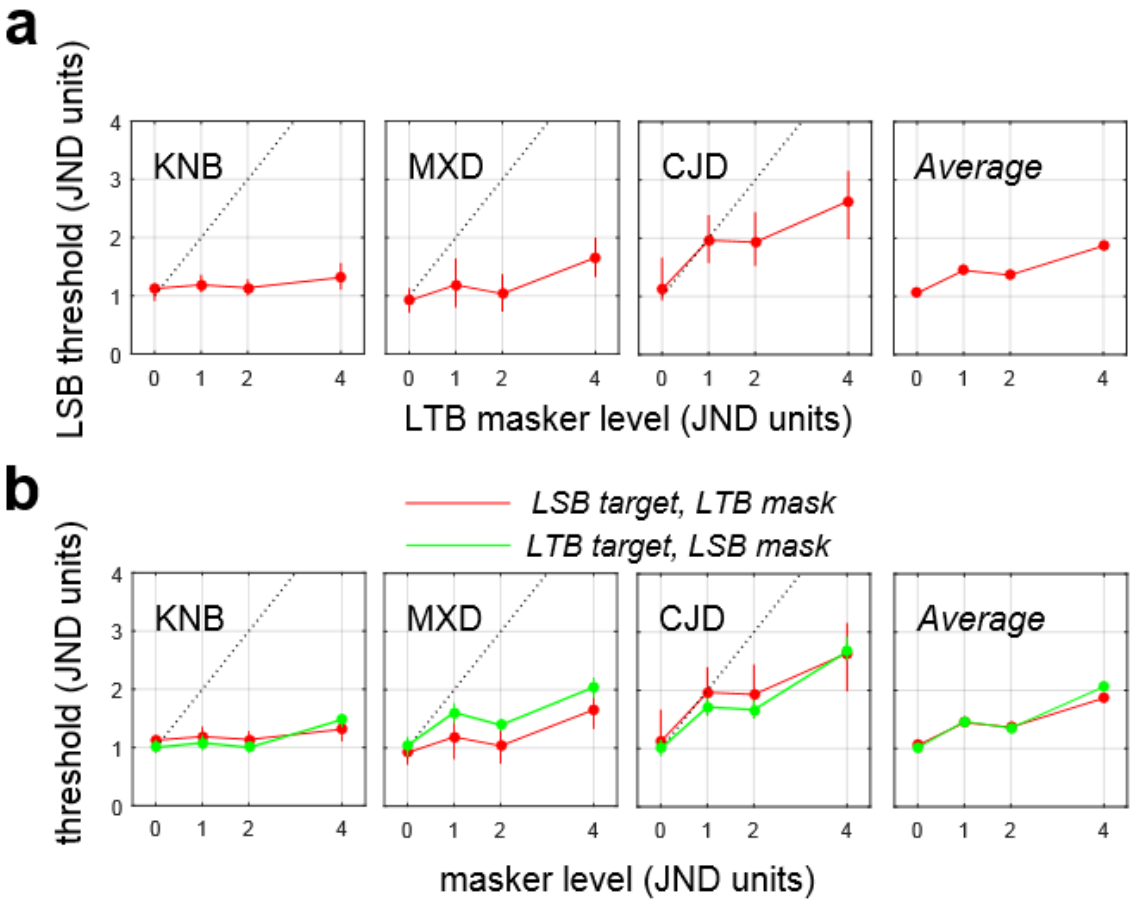
a
LSB threshold (JND units)
KNB
MXD
CJD
Average
LTB masker level (JND units)
b
LSB target, LTB mask
LTB target, LSB mask
threshold (JND units)
KNB
MXD
CJD
Average
masker level (JND units)

FIGURE 6

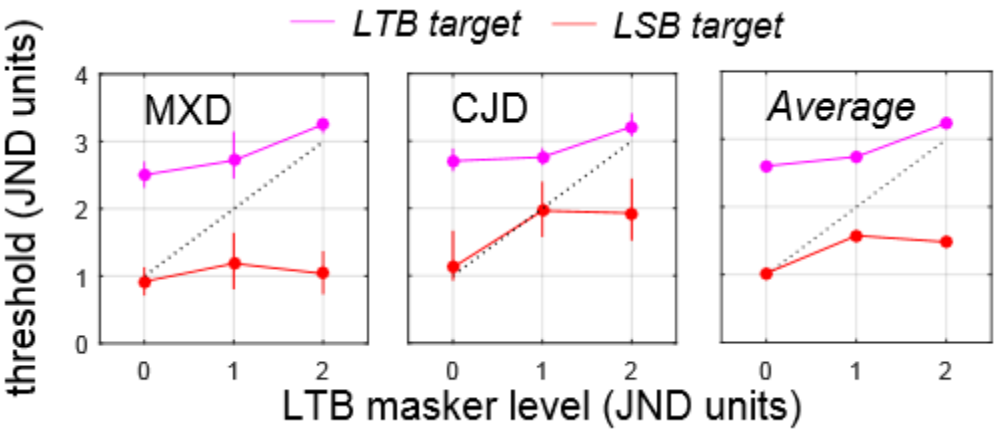
LTB target
LSB target
threshold (JND units)
MXD
CJD
Average
0
1
2
3
4
LTB masker level (JND units)

FIGURE 7

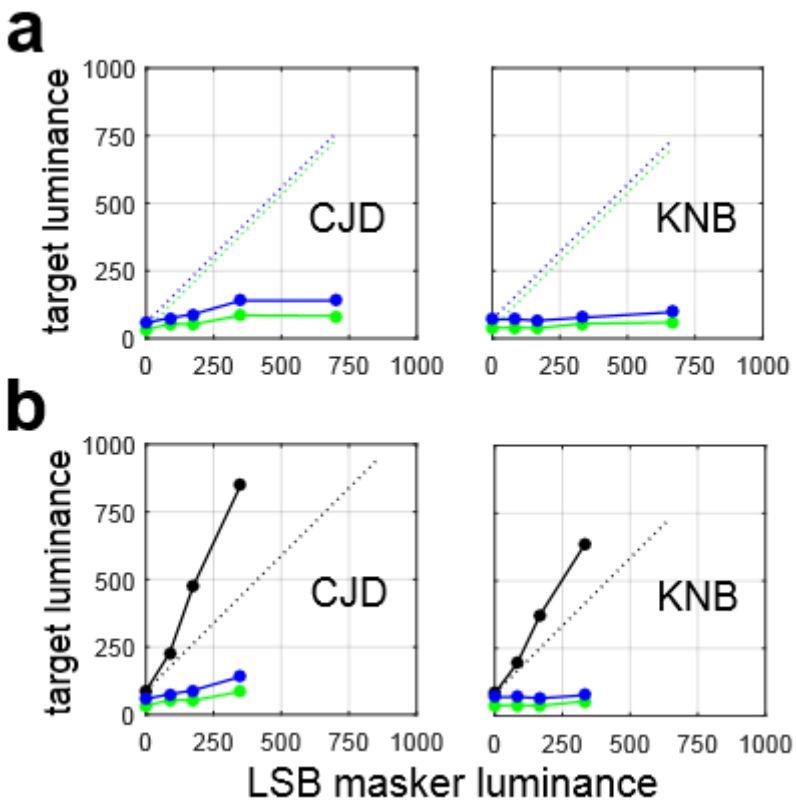
a
b
target luminance
LSB masker luminance
CJD
KNB
0
250
500
750
1000

FIGURE 8

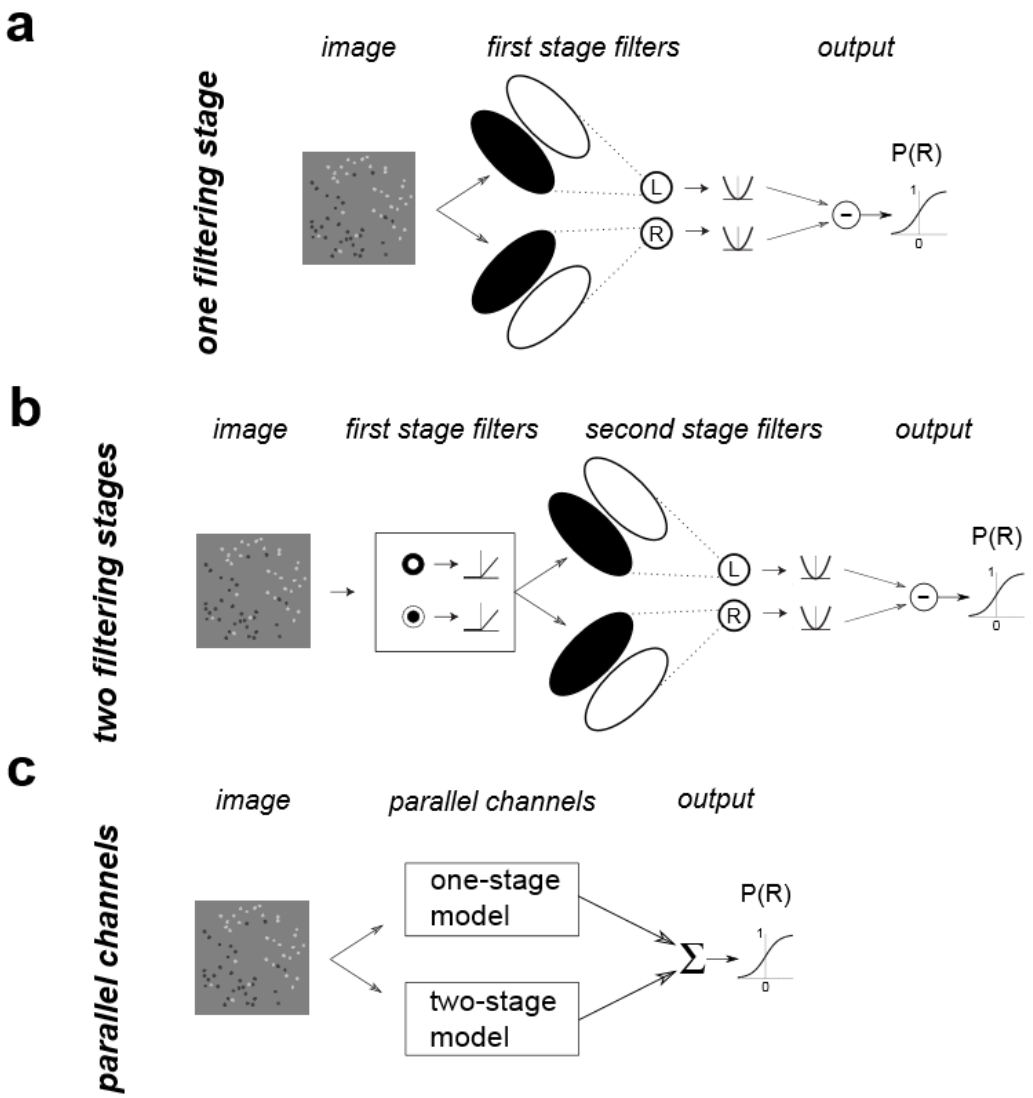
a
one filtering stage
image
first stage filters
output
P(R)
L
R
1
0
b
two filtering stages
image
first stage filters
second stage filters
output
P(R)
L
R
1
0
c
parallel channels
image
parallel channels
output
one-stage model
two-stage model
P(R)
Σ
1
0